Injection Locking Performance of a 41-GHz 10-W Power Combining Amplifier

DALE W. MOONEY, MEMBER, IEEE, AND FRANKLIN J. BAYUK, MEMBER, IEEE

Abstract—**Due to the ever growing and tremendous demand for satellite communications channels, and the resultant spectrum crowding, there is an increasing interest in developing hardware appropriate for communication satellite use in the EHF frequency spectrum. Even with the advent of the space shuttle, reliability is still of paramount importance for hardware intended for satellite applications. While the traveling-wave tube (TWT) is presently the industry workhorse for satellite downlink transmitter use, their poor record of reliability becomes even worse as the operating frequency is increased from 4 GHz to 12 GHz, 30 GHz, 40 GHz, and beyond. For this reason and also the greater simplicity, particularly in the power supply requirements, attention is naturally directed toward a solid-state replacement for the TWT. This paper details the measured performance of a solid-state amplifier which delivers 10 W of RF output power at an operating frequency of 41 GHz. The development of this amplifier is a significant milestone toward building a space-qualified high-power solid-state transmitter for spacecraft use.**

I. Introduction

SILICON DOUBLE-drift diodes have been employed in the development of a 10-W solid-state amplifier operating at 41 GHz [1], [2]. The key component of this amplifier is a 12-diode resonant rectangular cavity combiner. This performance is a state-of-the-art value representing the highest frequency, highest solid-state power achieved to date. The development activity involved a variety of disciplines including device characterization, circulator design, multiple-diode circuit design, and amplifier integration and test.

II. Approach

The primary specifications of frequency (41 GHz), power (10 W), bandwidth (100 MHz), gain (30 dB), and efficiency (10 percent) were used to establish a two-stage amplifier design which would simultaneously satisfy these requirements. Fig. 1 illustrates schematically the gain and power distribution which led to state-of-the-art results. This configuration, consisting of a multiple-junction circulator module, a driver module, and a combiner module, established the foundation for the milestone activities of device characterization, multiple-junction circulator development, driver and combiner module development, noise characterization, RF test, and reliability projection.

The two-stage amplifier consists of a single-diode driver stage operating in a TE_{101} resonant cavity, and a twelve-diode TE_{106} rectangular resonant-cavity power-combining structure [3].

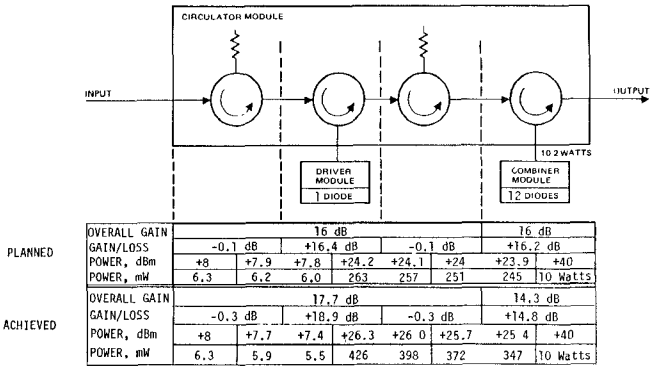

PLANNED	OVERALL GAIN	16 dB					16 dB	
	GAIN/LOSS	-0.1 dB	+16.4 dB		-0.1 dB		+16.2 dB	
	POWER, dBm	+8	+7.9	+7.8	+24.2	+24.1	+24	+23.9	+40
	POWER, mW	6.3	6.2	6.0	263	257	251	245	10 Watts
ACHIEVED	OVERALL GAIN	17.7 dB					14.3 dB	
	GAIN/LOSS	-0.3 dB	+18.9 dB		-0.3 dB		+14.8 dB	
	POWER, dBm	+8	+7.7	+7.4	+26.3	+26 0	+25.7	+25 4	+40
	POWER, mW	6.3	5.9	5.5	426	398	372	347	10 Watts

Fig. 1. 41-GHz 10-W amplifier design.

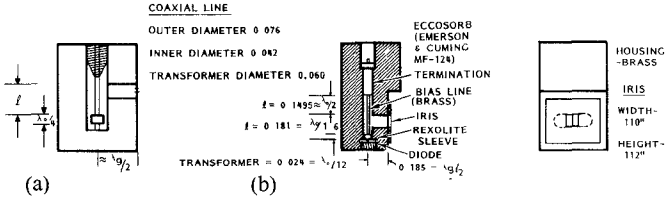

Fig. 2. Driver amplifier design parameters. (a) Classic Kenyon circuit. (b) 41-GHz driver amplifier circuit.

The single-diode driver amplifier consists of a coaxial cavity magnetically coupled to a waveguide cavity which is subsequently linked to the waveguide input–output interface by means of an inductive iris. The configuration of the amplifiers is similar to the classic "Kenyon" [4] type circuit. Fig. 2 presents the dimensional information pertinent to the actual design.

Departure from the classic circuit is noted in two areas: 1) the termination element is abrupt rather than tapered; and 2) the coaxial transformer is less than $\lambda_0/4$. These changes were made on the basis of theoretical projections of the bias-line impedance presented to the diode and the empirical data acquired by testing actual circuit designs. By removing the taper from the termination element, less power is lost which improves circuit efficiency. Using a flat-face termination, however, introduces a position-sensitive parameter. In most cases, a length of $\lambda_0/2$ from the waveguide cavity center line is an appropriate initial position. The length of the transmission line and the coaxial transformer are dependent on the impedance level that must be presented to the diode for a conjugate match

Manuscript received April 22, 1982; revised June 21, 1982. This work was sponsored and funded in part by AFWAL, Wright-Patterson Air Force Base, OH 45433, under Contract F33615-77-C-1185.

The authors are with the TRW Electronics and Defense Sector, One Space Park, Redondo Beach, CA 90278.

0018-9480/83/0200-0171$01.00 ©1983 IEEE

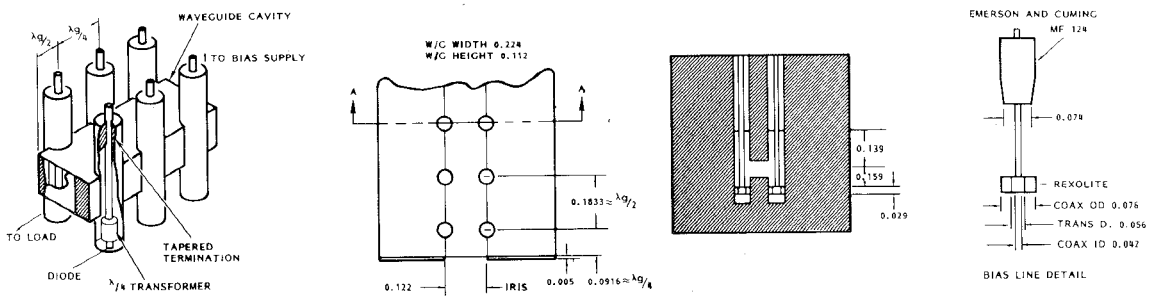

(a) (b)

Fig. 3. Power amplifier design parameters. (a) Classic presentation. (b) 41-GHz design.

condition. The 0.024-in transformer length is physically approximately $\lambda_0/12$ long; however, the dielectric sleeve increases the effective electrical length by a factor of $\sqrt{\epsilon_r}$, which in this case results in

$$\lambda_0/12 * \sqrt{2.56} \approx \lambda_0/8.$$

The exact dimensions were determined by iterating between the theoretical predictions and experimental results. Using different diodes or diodes in a different package will alter these coaxial dimensions accordingly. The waveguide cavity is defined by the iris and the back wall or shorting plane of the waveguide. A length consistent with $\lambda_g/2$ is appropriate for this design.

Fig. 3 presents design parameter information on the twelve-diode power amplifier. As with the single-diode circuit, departure from the classical circuit is noted. The distribution of the coaxial lines along the waveguide is altered from the theoretical $\lambda_g/2$ by approximately 2.5 percent. The addition of the coaxial scallops and the perturbation created by the coaxial center conductors affects the inherent resonant response of the waveguide cavity, and therefore it is necessary to compensate for this impact by decreasing or increasing the distance between center conductors along the broad wall of the waveguide. An approximation of the amount of compensation required can be determined by evaluating the resonant frequency of a cavity with the prescribed number of scallops and center conductors, and subsequently equating this to an unperturbed cavity. This equivalent cavity prescribes the coaxial line spacing for the desired resonant frequency.

The coaxial dimensions of the multiple-diode circuit are also shown to deviate from the classic circuit. The interactive loading of the coaxial circuits apparently affects the coupled impedance and, thus, a new set of transformations is required to present the appropriate conjugate impedance to the diode. As in the case of the single-diode driver, this is an iterative process between theoretical prediction and experimental results.

In the development of the amplifier, all bias lines were made identical in order to avoid an infinite select-in-test matrix. This approach is very functional, but may result in less than optimum performance if a wide variation in diode parameters is present. The diodes used in the development had been both dc and RF screened for uniformity in order to minimize these variations.

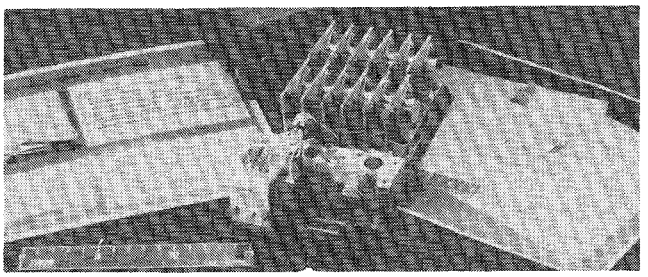

Fig. 4. Integrated amplifier assembly with cross-section pictorials.

The bias-line terminations in the twelve-diode circuit were also modified from the design used in the single-diode circuit. A totally flat termination configuration introduced spurious behavior due to the multiresonant waveguide circuit and the ability of the coaxial modules to selectively couple to more than one mode. A fully tapered termination results in extremely stable operation at the expense of excessive power loss. The final configuration was a partially tapered termination, as shown, which provided an acceptable compromise between efficiency and stable, nonspurious behavior.

Fig. 4 displays the fully integrated amplifier along with pictorials which provide cross-sectional details of both stages.

This amplifier development is part of a larger program for the development of a highly reliable millimeter-wave satellite communication system. The scope of this effort encompassed the design, fabrication, and evaluation of an EHF solid-state amplifier. The amplifier assembly is intended for internal mounting in a satellite transmitter. Because of the wide bandwidth achieved, the amplifier lends itself to a variety of space applications from a single high data rate user to multiple low data rate users.

III. Amplifier Evaluation

Due to the wide range of potential space applications and the selected mode of amplification, the completed amplifier was subjected to a series of operational and environmental tests. The operational tests serve to verify the applicability of the amplifier to a wide-band communications link. The environmental tests prove the survivability of the amplifier when subjected to the adverse environments encountered in satellite launch and operation.

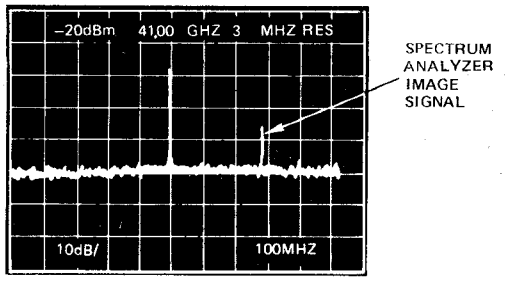

Fig. 5. Spectrum analyzer display for single-frequency locked amplification.

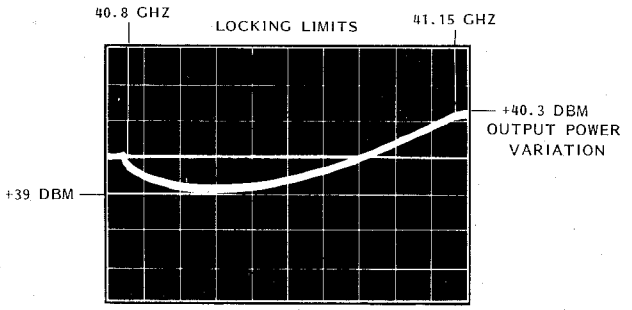

Fig. 6. Oscillographic baseband evaluation of the amplifier.

A. Noise Evaluation

Of major concern with any amplifier intended for communications use is the noise performance characteristic of that amplifier. In the case of an IMPATT amplifier, the predominant noise contributor is avalanche noise [5], [6]. Avalanche noise is the direct consequence of the ionization process which results whenever any charge carrier pair does not generate the expected single new carrier pair, but produces no new carrier pair or possibly two or more. The resulting fluctuations, random noise, are significant, particularly under high RF-voltage conditions present for an injection-locked oscillator. For this reason, it is expected that the injection-locked oscillator will have a higher effective noise figure than an equivalent stable negative-resistance amplifier. Since the amplifier is configured as an injection-locked oscillator, conventional noise-figure measurements are not applicable. This is because an injection-locked amplifier will produce full output power regardless of the input condition. Therefore, a noise-figure meter which switches a noise source at the input of the amplifier on and off would not be able to discern any difference at the amplifier output.

While conventional noise-figure measurement is precluded in the case of an injection-locked amplifier, other tests are available which fully characterize the amplifier's noise performance, such as RF spectrum analysis, oscillographic baseband observation, and Bit Error Rate (BER) measurement.

B. Spectrum Analysis and Baseband Evaluation

Fig. 5 is a photograph of the spectrum analyzer display of the amplifier output spectrum when locked up to a 41-GHz input signal. The low-level signal on the right is an image signal generated within the spectrum-analyzer external mixer. This data indicates that there were no discernable spurious signals within ± 500 MHz of the signal. By tuning the spectrum analyzer across the band, it was demonstrated that there were no spurious signals in the entire waveguide band, 33 to 50 GHz, verifying the coherent operation of the amplifier.

When the amplifier was swept across its locking range of 300 MHz, no spurious signals were detected within the resolution limit of the spectrum analyzer and external mixer of approximately 40 dB below the signal level.

The baseband observation of the amplifier output signal is shown in Fig. 6 where the locking limits and power variation are identified on the oscilloscope photograph. Both of these noise evaluation techniques were employed throughout the development of the amplifier to judge the quality of both the circuit-diode match and the effectiveness of the coaxial terminations utilized in the combiner structure.

C. Bit Error Rate Measurements

The purpose of the BER test was to measure probability of error (P_E) as a function of energy per bit to noise density ratio (E_b/N_0), the digital system equivalent of signal-to-noise ratio [7], [8]. This test compares the digital input signal to the digital output signal and effectively notes the difference in terms of a bit count. Any discrepancies are noted as a bit error. A pseudorandom cyclical bit generator is initiated at a chosen data rate with the type of modulation desired. The counter is used to establish the bit count and a comparison can be made between the reference of the input signal and the amplifier signal. BER tests are sensitive to detect group delay dispersion and amplitude response dispersion by measuring the degradation in the signal-to-noise ratio E_b/N_0.

The availability of both a 38-GHz, 5-W power-combining amplifier and the required upconversion–downconversion hardware from previous development efforts [9], [10] from the BER test system's baseband to *Ka*-band, provide the rationale for completing the tests without the need to duplicate the entire up and downconversion hardware at 41 GHz.

The tests were conducted at a data rate of 100 MBPS per channel resulting in a QPSK composite data rate of 200 MBPS.

The energy per bit to noise ratio can be defined as the carrier power to noise power plus a correction factor. The correction factor is necessary to take into account the difference between the noise bandwidth (B_N) and the signal or data bandwidth (DBW).

In equation form, these quantities are

$$\frac{E_b}{N_0} = \frac{C}{N_T} + CF, \qquad CF = 10\log_{10}\frac{B_N}{\mathrm{DBW}}.$$

For 100 MBPS/channel QPSK, the data bandwidth

DBW = 200 MHz. Therefore, the correction factor is

$$CF = 10\log_{10}\frac{B_N}{\text{DBW}} = 10\log_{10}\frac{515}{200} = 4.11 \text{ dB},$$

$$CF = 4.11 \text{ dB}.$$

Probability of error versus E_b/N_0 is plotted in Fig. 7 for the cases of *Ka*-band terminal, *Ka*-band terminal plus power driver (injection-locked), and *Ka*-band terminal plus power driver plus power-combining amplifier (injection-locked). Table I summarizes the degradation in BER for each element in the system. The degradation attributable to the power-combining amplifier was 0.2 dB or less over the range of 10^{-2} to 10^{-6} BER. Knowing the power (hence gain) levels at each stage and that the Q_{ext} for the combiner is 30, the locking bandwidth for the combiner was calculated to be approximately 400 MHz. This is roughly two times the composite data bandwidth of 200 MHz.

Theoretically, the energy in a phase shift key (PSK) modulated signal is contained in an infinitely wide bandwidth. In practice, a much narrower, finite, bandwidth is adequate. As an example, for QPSK, roughly 90 percent of the signal energy is contained within a bandwidth equal to the composite data rate, in this case 200 MHz [11]. To faithfully reproduce this signal, an amplifier bandwidth of 200 MHz would be adequate, *provided* the phase response of the amplifier was flat over the entire 200 MHz. As this is not usually the case, additional amplifier bandwidth is required to assure a phase flat 200-MHz bandwidth. In the case of the injection locked amplifier evaluated, a 2:1 bandwidth ratio was proven to be adequate for satisfactory BER performance.

The results obtained at 38 GHz are representative of the performance of the 41-GHz amplifier and indeed any similar multidiode resonant-cavity injection-locked amplifier.

Both AM and phase noise were measured for three configurations. The first measurement was conducted with the 10-W amplifier injection-locked to a low-noise 41-GHz Gunn source. In the second measurement, the 41-GHz Gunn oscillator was turned off and the 10-W amplifier was allowed to free run. Finally, the 10-W amplifier was removed and noise measurements were conducted on the 41-GHz low-noise Gunn oscillator.

Comparing the results of the three phase noise measurements reveals that the free-running 10-W IMPATT amplifier has a typical noise level 10–12 dB higher than that of the low-noise Gunn oscillator. When the 10-W amplifier is injection-locked to the low-noise Gunn source, the phase noise for the combination is the same as for the Gunn oscillator alone. This indicates that the noise characteristics of the locking source (Gunn oscillator) dictates the phase noise performance of the injection-locked amplifier.

The AM noise for the free-running 10-W amplifier was approximately 10–20 dB higher than for the low-noise Gunn oscillator. When injection locked to the Gunn oscillator, the AM noise for the 10-W amplifier was 5–10 dB lower than for the free-running 10-W amplifier.

As predicted by injection-locking theory, [12]–[14], the phase noise performance of the 10-W injection-locked amplifier is a faithful reproduction of the phase noise characteristic of the driving signal. The AM noise performance of the driving signal is degraded by approximately 5–10 dB by the 10-W, 30-dB gain IMPATT amplifier.

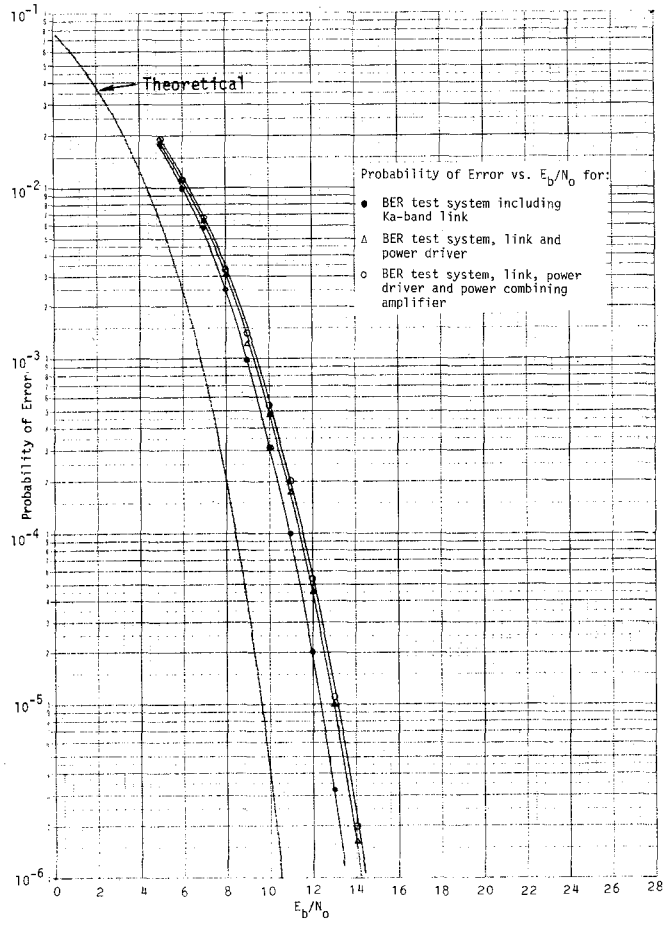

Fig. 7. Composite BER test data.

TABLE I
POWER COMBINING AMPLIFIER BER PERFORMANCE

	Degradation from Ideal (dB)		
BER	Test System	Power Driver	Combiner
10^{-2}	1.7	0.1	0.1
10^{-3}	2.3	0.3	0.1
10^{-4}	2.6	0.4	0.2
10^{-5}	2.8	0.7	0.1
10^{-6}	3.1	0.7	0.2

The results of these various noise evaluation techniques (BER, spectrum analysis, baseband analysis, and close in phase and AM noise) indicate that an injection-locked, multidiode IMPATT amplifier is properly suited for amplifying PSK modulated signals in a spacecraft communications link.

IV. Environmental Tests

The completed 10-W 41-GHz solid-state amplifier was subjected to a limited series of environmental tests. The purpose of these tests was to verify the survivability of the

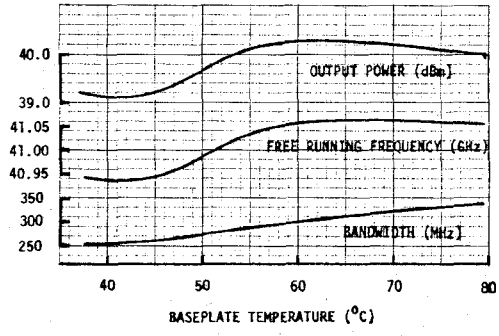

Fig. 8. Amplifier output power, free-running frequency, and bandwidth as a function of baseplate temperature.

TABLE II
TEMPERATURE TEST DATA

#0 Diode Plate (°C)	#1 Base Plate (°C)	#2 Base Plate (°C)	#3 Driver (°C)	#4 Combiner (°C)	F_o (GHz)	P_o (dBm) Free-Run.	BW (MHz)	Telem (Volts)
	24.2	37.3	28.4	38.7	40.95	39.2	254	3.816
37.6	39.3	53.3	45.8	55.2	41.02	40.16		3.841
65.3	46.3	60.7	50.8	62.0	41.06	40.36	304	3.851
83.3	65.9	79.1	69.8	80.9	41.06	40.06	348	3.905
49.6	30.1	45.2	40.1	48.2	40.94	39.2	259	3.851

amplifier when subjected to some of the environmental extremes that would be encountered on a spacecraft. The first of the two tests that were conducted was operation over an extended temperature range. After successful completion of the temperature test, the amplifier was subjected to vibration for simulation of a spacecraft launch environment.

A. Temperature Test

The amplifier was subjected to temperature changes by allowing the baseplate to deviate from 37°C to 79°C. Table II and Fig. 8 compare the output power, free-running frequency, and locking bandwidth as a function of baseplate temperature.

B. Vibration Test

The amplifier was subjected to a random vibration in three axes to verify spacecraft launch survivability. During vibration, telemetry was monitored to verify bias-line continuity. The data acquired gave no indication of interrupted bias current, and thus verified the design integrity from a dc perspective. After completion of the vibration test, the amplifier was evaluated in terms of the RF performance. A frequency shift of 120 MHz was noted; however, the power and bandwidth performance were unchanged. The change in frequency was traced to slight movement in the dielectric sleeve which surrounds the bias line in the driver stage. This sleeve was returned to its proper position, and nominal performance was again observed.

V. RELIABILITY

A spacecraft amplifier is typically specified to have an operational lifetime of 10 years. With the basic structural integrity of the amplifier defined as indicated by survivable

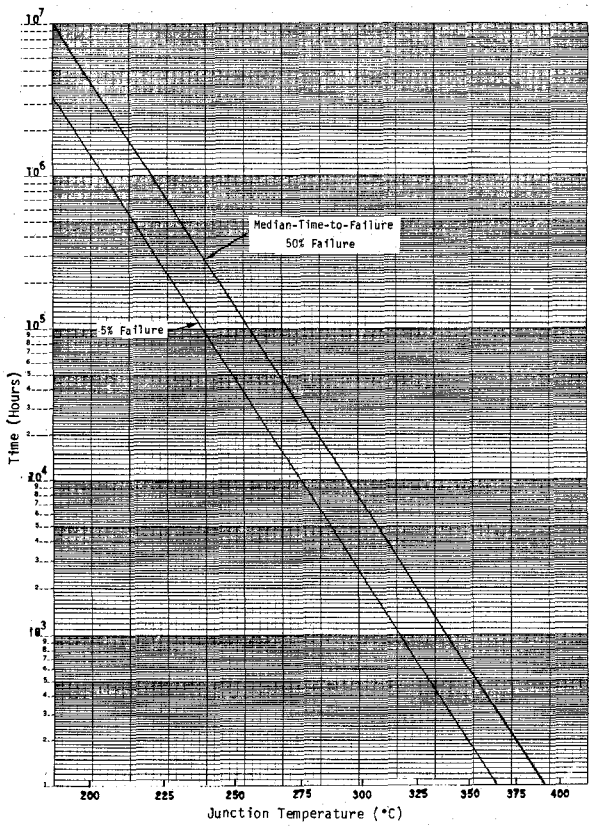

Fig. 9. IMPATT diode life test reliability projections.

thermal and vibration testing, the main-lifetime limiting factor for a solid-state IMPATT amplifier is the IMPATT diode. The primary parameter in this regard is the diode-junction temperature.

Accumulation of diode lifetime data by accelerated temperature aging is a continuous activity at many companies to determine reliable junction temperature criteria. Lifetime data appropriate to the diodes employed in the 10-W, 41-GHz amplifier is presented in Fig. 9 [15]. Plotted as a function of junction temperature in degrees Celsius are median time-to-failure (MTTF) and time to 5-percent failure.

The probability of a mission success can be calculated based on the cumulative failure rates of the individual components. Table III shows the part failure rates used for the current regulator. The rates are obtained from MIL-HDBK-217, Revision C, based on a 30°C ambient temperature and a stress ratio of 20 percent for all parts. The total current regulator failure rate is 107.25 per 10^9 h. There are 13 regulators employed in the amplifier. The waveguide circulator, of which there are four, has been assigned a failure rate of 10 per 10^9 h. These component failure rates, in conjunction with the reliability projection data of Fig. 9, are used to calculate the probability of mission success, which will be a function of diode-junction temperature. Three mission profiles were considered: a 10-year mission at 100-percent duty cycle; a 3-year mission at 100-percent duty cycle, which is the same as a 10-year mission at 30-percent duty cycle; and a 3-year mission at 30-percent duty cycle. For each of these mission profiles, two amplifier configurations were evaluated. The first configuration

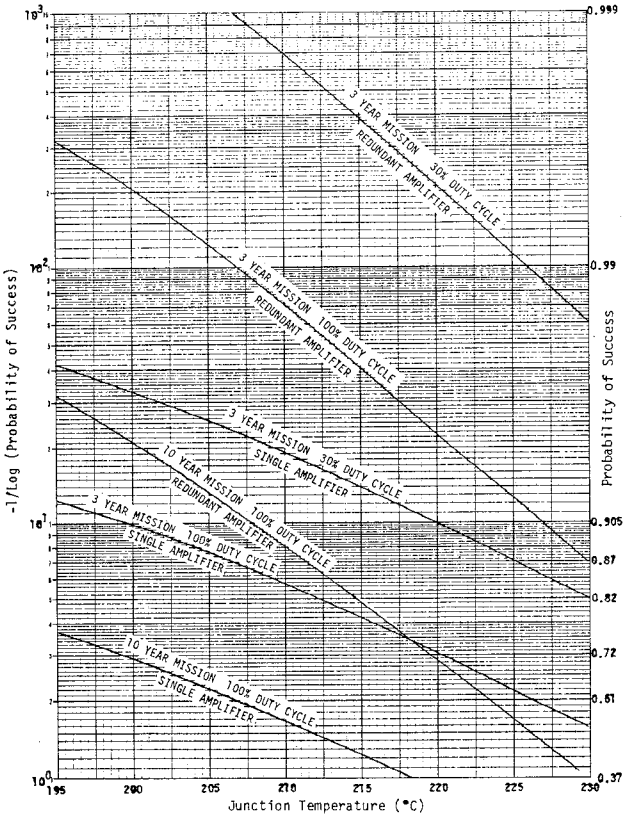

Fig. 10. Probability of mission success.

TABLE III
CURRENT REGULATOR PART FAILURE RATE SUMMARY

Part	Number Used	$\lambda 10^{-9}$	$N\lambda 10^{-9}$
IC, Linear, LM117K (26T)	1	5.412	5.412
Diode, Zener	1	1.080	1.080
Resistor, RNC 55	2	0.002	0.004
Resistor, RCR 20	1	0.008	0.008
Resistor, RTR, Variable	1	0.720	0.720
Capacitor, CKR06	1	0.025	0.025
Fuse	1	100.0	100.0
TOTAL			107.25

is a single amplifier as built and tested. Also examined is a redundant amplifier configuration. If a part in one amplifier fails, the backup amplifier takes over to complete the mission. Probability of mission success as a function of junction temperature for the six cases evaluated are plotted in Fig. 10.

The implication of this reliability projection is that a redundant amplifier chain is required to achieve a greater than 90-percent probability of success for a 10-year 100-percent duty cycle orbital mission. In addition, a junction temperature of 208°C or lower must be maintained.

VI. CONCLUSIONS

The development of a solid-state amplifier at 41 GHz has resulted in a unit which is capable of delivering 10 W of output power at a 32-dB gain over 250 MHz of bandwidth with an overall dc to RF conversion efficiency of 6.8 percent. The amplifier was tested in a traditional laboratory setting during the development phase. After the hardware was integrated, limited environmental tests were performed. The results of the development and environmental tests indicate that substantial progress has been made in defining the necessary ingredients for fabricating a highly reliable solid-state amplifier suitable for satellite communications systems.

ACKNOWLEDGMENT

The authors wish to thank J. E. Raue for his contributions in the initiation of the program and the many subsequent helpful and motivating discussions.

REFERENCES

[1] D. W. Mooney and F. J. Bayuk, "EHF solid-state amplifier," TRW Defense and Space Systems, Rep. AFWAL-TR-81-1100, Sept. 1981.
[2] D. W. Mooney and F. J. Bayuk, "Power-combining produces benchmark 41-GHz amplifier," *Microwave Systems News*, vol. 12, no. 7, pp. 88–105, July 1982.
[3] K. Kurokawa, "The single-cavity multiple-device oscillator," *IEEE Trans. Microwave Theory Tech.*, vol. MTT-19, pp. 793–801, Oct. 1971.
[4] N. D. Kenyon, "A circuit design for millimeter-wave IMPATT oscillators," in *1970 G-MTT Symp. Dig.*, pp. 300–303.
[5] S. M. Sze, *Physics of Semiconductor Devices*. New York: Wiley Interscience, 1969, pp. 130–131.
[6] A. Van Der Ziel, *Fluctuation Phenomena in Semiconductors*. New York: Academic, 1959.
[7] K. Feher, *Digital Communications: Microwave Applications*. Englewood Cliffs: Prentice-Hall, 1981, pp. 21–25.
[8] F. G. Stremler, *Introduction to Communication Systems*. Boston, MA: Addison-Wesley, 1977, pp. 461–490.
[9] F. J. Bayuk and J. E. Raue, "*Ka*-Band solid-state power amplifier," in *1977 IEEE-MTT Int. Symp. Dig.*, pp. 29–31.
[10] D. L. Lochhead, "Wideband digital transmitter/receiver," TRW Defense and Space Systems, Rep. RADC-TR-77-261, Aug. 1977.
[11] J. J. Spilker, *Digital Communications by Satellite*. Englewood Cliffs: Prentice-Hall, 1977, pp. 305–324.
[12] L. J. Paciorek, "Injection locking of oscillators," *Proc. IEEE*, vol. 53, pp. 1723–1727, Nov. 1965.
[13] R. Adler, "A study of locking phenomena in oscillators," *Proc. IEEE*, vol. 61, pp. 1380–1385, Oct. 1973.
[14] K. Kurokawa, "Noise in synchronized oscillators," *IEEE Trans. Microwave Theory Tech.*, vol. MTT-16, pp. 234–240, Apr. 1968.
[15] M. Morishita and E. Nakaji, "EHF silicon double drift IMPATTS," Hughes Aircraft Company, Final Tech. Rep. AFWAL-80-1178, Dec. 1980.

✤

Dale W. Mooney (S'74–M'78) was born in Bakersfield, CA in 1955. He received the B.S. degree in electronic engineering from California Polytechnic State University in San Luis Obispo, CA.

He has been a Member of the Technical Staff at TRW Electronics and Defense in Redondo Beach, CA since 1977. He has been involved in the design, evaluation, and testing of IMPATT circuits, particularly multidiode power-combining amplifiers applicable to high-power EHF transmitters. In addition, he has been involved with work on wideband up and down converters in the EHF frequency spectrum.

Mr. Mooney is a member of Tau Beta Pi, Eta Kappa Nu, and Phi Kappa Phi, and is presently pursuing the M.S. degree in electrical engineering at the University of Southern California.

Franklin J. Bayuk (S'70–M'71) was born in Greenwood, WI on Feb. 21, 1945. He received the B.S. degree in electrical engineering technology from the Milwaukee School of Engineering in 1971, and the M.S. degree in electrical engineering from Loyola Marymount University in 1975.

Since 1972 he has been a Member of the Technical Staff at TRW Electronics and Defense in Redondo Beach, CA. He is currently an acting Section Head in the Millimeter-Wave Technology Department and is a member of the Senior Technical Staff. His previous assignments included direct responsibility for work on millimeter-wave solid-state power-combining amplifiers, multipliers, upconverters, and down-converters. In addition, he has had direct responsibility for company sponsored work on millimeter-wave waveguide components. This work included design of multiple-section waveguide bandpass filters, band-reject filters, high-pass filters, waveguide-to-coaxial transitions, and various other passive structures in the 15 to 100 GHz frequency range. His present assignment encompasses a wide range of activities from responsible design engineering to the sub-project management function in support of systems engineering. In this role, he has accumulated experience with space qualification of hardware and system considerations involved with integration and testing of various subsystems.

Synchronization Effects in a Submillimeter Josephson Self-Oscillator

J.-C. HENAUX, G. VERNET, AND R. ADDE, MEMBER, IEEE

Abstract—**We present an experimental and theoretical study of injection-locking in an oscillator in the presence of noise. The experiment is performed with a Josephson point-contact self-oscillator heterodyne receiver irradiated by a very weak ≃ 1-THz signal. A general calculation of the oscillator response at low injection level is made based on the theoretical treatment of Stratonovitch. We show that the Josephson oscillator described by the RSJ model obeys the general locking equation in the presence of noise. We assume a simple evolution law of the oscillator spectrum as a function of detuning and calculate its response. The experimental results are compared with computer calculations and the implications are discussed.**

I. INTRODUCTION

WE STUDY HERE the partial synchronization of an oscillator in the presence of noise on a very weak external signal. We want more precisely to determine its spectrum as a function of the detuning relative to the injection frequency. The method of analysis does not depend on the type of oscillator. We present a theoretical and experimental study of synchronization in the superconducting Josephson self-oscillator mixer which is a system where noise effects are significant [1]. In this heterodyne mode of detection, a Josephson junction acts simultaneously as the local oscillator and as the nonlinear down-converter element. Our experimental interest is in applications of the device at submillimeter wavelengths with large frequency ranges of operation as may be required in a frequency-agile receiver. Therefore, the Josephson point-contact junction is coupled to a wide-band structure. In ths situation, noise plays a crucial role in the treatment of synchronization effects.

Injection locking in a Josephson point contact coupled to an X-band cavity was studied by Stancampiano and Shapiro [2] and Stancampiano [3]. In these experiments, noise was not considered since the junction was coupled to a high-Q resonator. The results could be interpreted on the basis of Adler's theory [4] of phase locked electronic oscillators because of the close similarity between the synchronization equations describing an electronic oscillator and the cavity-coupled Josephson oscillator.

For the wide-band Josephson self-oscillator mixer that we investigate here, Adler's theory cannot be applied since noise results in large natural oscillation linewidths [1]. We start from the general theoretical treatment of Stratonovitch [5] of injection in electronic oscillators in the presence of noise. This theory was used previously by Stephen [6] who calculated the effect of noise on the rounding of

Manuscript received May 19, 1982; revised, August 2, 1982.

The authors are with the Institut d'Electronique Fondamentale, Bat. 220, Université of Paris Sud, Orsay, France 91405 (A laboratory associated with the Centre Nationale de Recherche Scientifique, Paris.)

0018-9480/83/0200-0177$01.00 ©1983 IEEE